Defence Research and Development Canada | Recherche et développement pour la défense Canada

DEFENCE R&D DÉFENSE

Study of phase quantization effects on synthesized array factor having a main beam and a prescribed null

Mathieu Caillet, Michel Clénet, Yahia M. M. Antar

Defence R&D Canada – Ottawa

Technical Memorandum

DRDC Ottawa TM 2008-291

December 2008

Canada

Study of phase quantization effects on synthesized array factor having a main beam and a prescribed null

Mathieu Caillet
Royal Military College of Canada

Michel Clénet
Defence R&D Canada – Ottawa

Yahia M. M. Antar
Royal Military College of Canada

Defence R&D Canada – Ottawa

Technical Memorandum

DRDC Ottawa TM 2008-291

December 2008

Co-author

Original signed by Michel Clénet

Michel Clénet

Approved by

Original signed by Bill Katsube

Bill Katsube
SH CNEW

Approved for release by

Original signed by Pierre Lavoie

Pierre Lavoie
Chairman DRP

Abstract

This document reports on investigations into the radiation characteristics of linear arrays with half-wavelength element spacing and digital phase shifters for an array factor having a main beam and a prescribed null. The weights of each element have been computed using the Minimum Variance Distorsionless Response method. In the considered scenario, the main beam is fixed and the prescribed null angular position varies between 1 and 60°.

Different results are presented here, first for exact phase and different number of elements. The main beam angular position is shifted and the half-power beamwidth drops when the prescribed null is below the position of the first natural null of the array factor without prescribed null. The prescribed null depth curve presents maxima and minima whose angular positions correspond to the sidelobes and natural nulls of the array factor without prescribed null, respectively. Moreover, the depth envelope of the prescribed null maxima is related to the level of the sidelobes of the array factor without prescribed null.

Based on these facts, the effect of phase quantization are studied. In particular, one can observe that the main beam angular position and half-power beamwidth errors are negligible. However, phase quantization affects the prescribed null position and depth. The larger the phase error, the greater the effect on the radiation pattern characteristics.

Résumé

Le présent document porte sur l'étude des caractéristiques de rayonnement de réseaux d'antennes linéaires, dont les éléments sont espacés d'une demi-longueur d'onde et sont munis de déphaseurs numériques, pour la synthèse d'un facteur de réseau comprenant un faisceau principal et un nul désiré. La pondération de chaque élément a été calculée au moyen de la méthode de réponse à variance minimale sans distorsion. Dans le scénario étudié, le faisceau principal est fixe tandis que la position angulaire du nul désiré varie entre 1° et 60°.

Différents résultats sont présentés, en commençant d'abord avec une phase exacte et pour plusieurs nombres d'éléments. Lorsque la position du nul désiré est inférieur à celle du premier nul naturel du facteur de réseau sans nul désiré, la position angulaire du faisceau principal est décalée et l'ouverture à mi-puissance du faisceau diminue. La courbe de profondeur du nul désiré présente des maximums et des minimums dont les positions angulaires correspondent respectivement aux lobes secondaires et aux nuls naturels du facteur de réseau sans nul désiré. De plus, l'enveloppe des maximums de la profondeur du nul désiré est liée au niveau des lobes secondaires du facteur de réseau sans nul désiré.

Basés sur ces constatations, les effets de la discrétisation de phase sont étudiés. Il est notamment possible d'observer que les erreurs sur la position angulaire du faisceau principal et la largeur de faisceau à mi-puissance sont négligeables. La discrétisation de phase influe cependant beaucoup sur la position et la profondeur du null désiré. Plus l’erreur de phase est élevée, plus cet effet est marqué.

Executive summary

Study of phase quantization effects on synthesized array factor having a main beam and a prescribed null

Mathieu Caillet, Michel Clénet, Yahia M. M. Antar; DRDC Ottawa TM 2008-291; Defence R&D Canada – Ottawa; December 2008.

Background: Phased array antennas are currently used in various applications such as radar and communication systems. Smart antennas are an interesting solution to overcome the interference issues in wireless communication or to cancel an unwanted signal. The array factor synthesis including interference rejection can be implemented either using digital phase shifters and amplifiers or employing analog to digital converters and digital processor. In both cases, complex weighting is generated and phase quantization introduces errors that directly impact the performance of the array. Thus, it is important to study the effect of the phase quantization to properly design smart antenna systems.
This report proposes an investigation into phase quantization effect on synthesized array factor having a main beam and a prescribed null. The used antenna array is linear with half-wavelength element spacing and digital phase shifters on each element. PAASoM, a analysis software tool developed by DRDC Ottawa for phased antenna array, has been used for this study.

Principal results: Considering a 16-element linear array with ideal phase shifters, two important outcomes can be addressed regarding the characteristics of an array factor having a main beam and a prescribed null varying between 1 and 60°. First, the main beam angular position is shifted and the half-power beamwidth drops when the prescribed null is below the position of the first natural null of the array factor without prescribed null. Second, the prescribed null depth curve is presenting some maxima and minima whose angular positions correspond to the sidelobes and natural null of the array factor without prescribed null, respectively.

Using the results obtained with perfect phase as reference, the phase quantization effects have been investigated considering the Root Mean Square (RMS) of the phase error as the analysis criteria. It has been noticed that the direction and half-power beamwidth of the main beam are similar to those with exact phase, except when the phase error is important; the results are slightly different in this case. However, the position and depth of the prescribed null are both affected by the phase quantization. The larger the phase error, the greater the effect on the radiation pattern characteristics. For instance, the prescribed null angular position can present an error up to 4.4° and the null depth an error around 60° when the average phase error RMS is 6.2°.

Significance of results: To the knowledge of the authors, only few studies have focused so far on the phase quantization effect in the case of prescribed nulls. Moreover, the non-conventional 2D colour representation available in PAASoM is useful in this investigation since it allows the visualization of the array factor as a function of a parameter, in particular the prescribed null position in this work. Interesting results not previously discussed in the literature have been compiled in this report. These results are promising for future investigations considering similar contexts. The results will impact on the design of phased arrays with digital components.

Future work: Future work will concern the investigation into phase quantization effects for arrays of various geometries as well as for scenarios with multiple beams and nulls. Only linear arrays have been considered in this study and results by considering other array geometries would be of interest. The same is true of multiple beams and nulls since one beam and one null have been investigated here, and realistic scenarios assume more than one beam and/or null. The study presented in this paper concerns only scenarios with a desired beam and a prescribed null. The obtained results can not be generalized for scenarios with multiple beams and nulls.
New analysis methods and functions implemented in PAASoM to realize this work and enhance the capabilities of the software will be useful for future studies.

Sommaire

Study of phase quantization effects on synthesized array factor having a main beam and a prescribed null

Mathieu Caillet, Michel Clénet, Yahia M. M. Antar ; DRDC Ottawa TM 2008-291 ; R & D pour la défense Canada – Ottawa ; décembre 2008.

Contexte : Les antennes réseau à commande de phase sont actuellement utilisées pour diverses applications, comme les systèmes radar et les systèmes de communication. Les antennes intelligentes sont une solution intéressante pour surmonter les problèmes d'interférences dans les communications sans fil ou pour annuler un signal non désiré. La synthèse d'un facteur de réseau prenant en compte la réjection d'interférence peut être réalisée au moyen de déphaseurs et d'amplificateurs numériques, ou encore à l'aide de convertisseurs analogique/numérique et d'un processeur numérique. Dans les deux cas, une pondération complexe est générée, et la discrétisation de phase introduit des erreurs qui influent directement sur les performances du réseau. Il est donc important d'étudier les effets de la discrétisation de phase pour bien concevoir les systèmes d'antennes intelligentes. Le présent rapport fait état d'une étude de l'effet de la discrétisation de phase sur la synthèse de facteur de réseau comportant un faisceau principal et un nul désiré. L'antenne réseau étudiée est linéaire et ses éléments sont espacés d'une demi-longueur d'onde ; chacun des éléments est muni d'un déphaseur numérique. PAASoM, un logiciel d'analyse des antennes réseau à commande de phase développé par RDDC Ottawa, a servi à cette étude.

Résultats principaux : En considérant un réseau linéaire de 16 éléments muni de déphaseurs idéaux, deux conclusions importantes peuvent être adressées sur les propriétés d'un facteur de réseau ayant un faisceau principal fixe et un nul désiré dont la position varie entre 1° et 60°. Premièrement, lorsque la position du nul désiré est inférieur à celle du premier nul naturel de la facteur de réseau sans nul désiré, le faisceau principal est décalé et l'ouverture mi-puissance diminue. Deuxièmement, la courbe de profondeur du nul désiré présente des maximums et des minimums dont les positions angulaires correspondent respectivement aux lobes secondaires et aux nuls naturels du facteur de réseau sans nul désiré.

En se servant des résultats obtenus avec des déphaseurs idéaux comme référence, les effets de la discrétisation de phase ont été étudié en utilisant la moyenne quadratique de l'erreur de phase comme critère d'analyse. Il a été observé que la direction et l'ouverture à mi-puissance du faisceau principal sont similaires à celles obtenues avec des déphaseurs idéaux, sauf lorsque l'erreur de phase est grande ; dans ce cas, les résultats sont légèrement différents. La discretisation de la phase a cependant un effet plus marqué sur la position et la profondeur du nul désiré. Plus l'erreur de phase est grande, plus cet effet est important.

Ainsi, lorsque la moyenne quadratique de l'erreur de phase est de 6,2°, la position angulaire du nul désiré peut présenter une erreur allant jusqu'4,4° et sa profondeur une erreur d'environ 60 dB.

Portée des résultats : A la connaissance des auteurs, seulement quelques études ont traité de l'effet de la discretisation de la phase jusqu'à présent dans le cas de la synthèse de facteur de réseau avec nul(s) désiré(s). De plus, la représentation non conventionnelle en 2 dimensions couleur offerte par PAASoM est utile à cette étude puisqu'elle permet de visualiser le facteur de réseau en fonction d'un paramètre, notamment par rapport à la position du nul désiré. Des résultats intéressants n'ayant pas été rapporté dans la littérature ont été rassemblés dans ce rapport. Ces résultats sont prometteurs pour de futures études sur des systèmes similaires, et ils auront leur importance sur la conception des réseaux à commande de phase au moyen de composantes numériques.

Perspectives : Les travaux futurs porteront sur l'étude des effets de la discrétisation de phase pour différentes géométries de réseaux et dans des scénarios comportant plusieurs faisceaux et plusieurs nuls. En effet, la présente étude ne concerne que les réseaux linéaires, et il serait intéressant d'obtenir des résultats en considérant d'autres géométries de réseau. Il en va de même pour plusieurs faisceaux et plusieurs nuls, car le scénario étudié ici ne comporte qu'un seul faisceau et un seul nul, alors que les scénarios réalistes en comportent davantage. La présente étude ne porte que sur des cas à un seul faisceau principal et à un seul nul désiré. Les résultats obtenus ne peuvent être généralisés à des cas comportant plusieurs faisceaux ou plusieurs nuls. Les études futures seront facilitées grâce aux nouvelles méthodes et fonctions d'analyse mises en oeuvre dans PAASoM pour réaliser ce travail et augmenter les capacités du logiciel.

Table of contents

List of figures

1 Introduction

Phased array antennas are currently used in various applications such as radar and communication systems. Advances in technology and mass production of integrated devices (for instance FPGA, DSP, ...) have made these latter cheaper and accessible for many uses. Smart antennas are an interesting solution to overcome the interference issues in wireless communication or to cancel an unwanted signal.

The array factor synthesis including interference rejection can be implemented either using digital phase shifters and amplifiers or employing analog to digital converters and digital processor. In both cases, complex weighting is generated and phase quantization introduces errors that directly impact the performance of the array. Thus, it is important to study the effect of the phase quantization to properly design smart antenna systems.

This report proposes an investigation into phase quantization effect on synthesized array factor having a main beam and a prescribed null. The used antenna array is linear with half-wavelength element spacing and digital phase shifters on each element. The investigation context and the analysis tool used for this work are presented in Section 2. Results with perfect phase are provided in Section 3 and then the effect of phase quantization on the beam and null characteristics are reviewed in Section 4. Conclusions and perspectives are given in Section 5.

2 Investigation context and used analysis tool

Several methods have been described in the literature to achieve null-steering [1]. Among these ones, the control of the amplitude of the element excitation has been proposed by D. S. Hicks [2] for linear arrays. Genetic algorithm has been used by W.-P. Liao et al. [3] to steer nulls in planar arrays by controlling the the current amplitude only. Another way to place nulls in the array factor of an antenna is to control the phase of each element. This method is interesting as digital phase shifters only can be employed to implement it [4]. For large phase perturbation, numerical solution is required. Furthermore, full amplitude/phase control can be used to steer prescribed nulls [5]. This method is quite flexible compared to the first two, and the weights are generated using linear systems. Finally, element position perturbation allows the steering of nulls [6].
In this section, the chosen method and conditions are presented, as well as the selected scenario and the analysis tool.

2.1 Chosen methods and conditions

The selected method is a full amplitude/phase technique, called Minimum Variance Distorsionless Response (MVDR) proposed by S. P. Applebaum in 1976. The weight computation relies on the power of the desired signals and interferences, and the maximization of the output Signal to Noise Ratio. Pattern synthesis with multiple-beam and/or multiple-null is possible, and only the desired signal directions have to be known. Fast computation of the weights is available using the Sample Matrix Inversion (SMI).

The assumed conditions for the desired and unwanted signals are the following:

- Signal to Noise Ratio (SNR) of 10 dB,
- Interference to Noise Ratio (INR) of 20 dB,
- Thermal Noise of -110 dBm,
- Weights computed at a single frequency.

These conditions corresponds to the case where the received power of the unwanted signal is above the thermal noise. Another method proposed by I. J. Gupta [7] can be used when the unwanted signal is below the thermal noise.

2.2 Selected scenario

In this study, a linear array with a constant half-wavelength element spacing has been considered. Moreover, the angular positions of the signals and weight quantization are:

- **One fixed desired signal** at boresight,
- **One scanning interference** away from boresight (1 to 60° in elevation),
- A weight is associated to each antenna element,
- The **amplitude** of each computed weight is **exact**,
- The **phase** of each computed weight is **quantized** using a digital phase shifter.

Fig. 1 presents the array geometry and the considered signals.

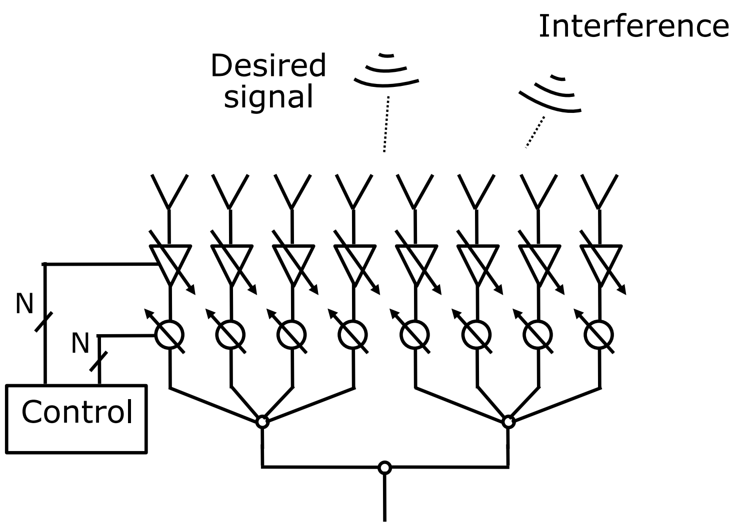

Figure 1: *Element array considered with desired and unwanted signals*

2.3 Analysis tool used for this study

A simulation tool has been developed by DRDC over the last few years to analyse the radiation characteristics of phased arrays using digital phase shifters. This software program, called PAASoM (Phased Array Antenna Software tool in Matlab) [8], allows the study of arrays of different geometries and lattices with the possibility of weighting each element in phase and magnitude. The elements can be grouped in sub-arrays, and each sub-array can have its own phase weighting. The array factor, which is defined as the sum of the weighted signals received by all the array elements (Eq. 2.1), can be calculated in one or several planes as a function of a parameter given by the user. This parameter can be the number of bits of the phase shifters, the scanning angles in azimuth and elevation or the frequency. For instance, effects of phase quantization on the array factor over scanning and frequency ranges have been underlined with PAASoM in [9].

$$AF(\theta,\varphi) = \frac{1}{N} \cdot \sum_{m=1}^{N} A_m e^{j\psi_m} e^{jk[x_m \cos(\varphi)\sin(\theta) + y_m \sin(\varphi)\sin(\theta) + z_m \cos(\theta)]} \quad (2.1)$$

where

- (x_m, y_m, z_m) are the Cartesian co-ordinates of the m^{th} antenna element,
- (A_m, ψ_m) are respectively the amplitude and the magnitude of the weight of the m^{th} antenna element,
- N is the number of antenna elements,
- (θ, φ) are the elevation and azimuth angles,
- k is the wave number.

Based on the version of this simulation tool that has been developed for conventional beam-forming (one beam only) [10] and on motivations presented earlier in the introduction, the implementation of additional methods has been realized in PAASoM to allow the synthesis of multi-beam and/or multi-null array factor. The additional methods contain diverse kinds of array processing methods, like the minimum-variance distortionless beamformer, also known as optimal beamformer [5], or the power inversion beamformer [11].

Several representations of the array factor or radiation pattern are available in PAASoM. A short example is given here to present the 1D conventional graph and the unconventional 2D colour developed in PAASoM. A 25-element linear array is considered, with the scan angle of the main beam as a parameter. The main beam is steering from 0 to 60° with a Chebyshev 30-dB amplitude distribution, and digital phase shifters are setting the phase at each antenna element. The 1D representation of the array factors in the plane containing the array with exact phase and 3-bit phase shifters is shown in Fig. 2 for the main beam angular position at 0, 10, 20, 30, 40, 50 and 60°. The effect of the phase quantization is clear, one can see an increase of the sidelobe level in Fig. 2(b) compared to the exact phase case.

Another way to represent the array factor is to consider the cuts of the array factor for all the parameter values and stack them on top of each other (Fig. 3). This representation allows good resolution for both the parameter values and elevation angles, and the quantization lobes can be very distinctively seen.

The 2D colour representation is very convenient to observe the effect of phase quantization over the scanning range and will be used in the following sections.

The assumed conditions, considered scenario and simulation tool have been presented in this section. Results with perfect phase for a desired signal and an interference are addressed in Section 3.

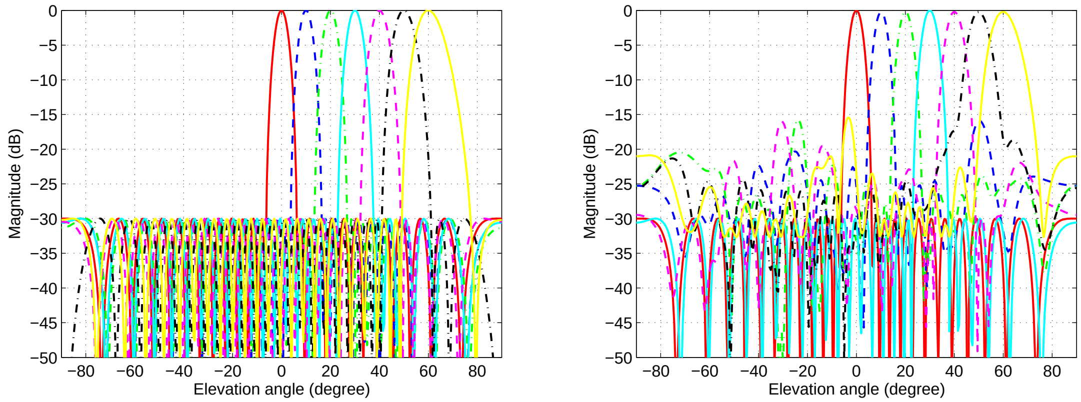

(a) (b)

Figure 2: *Array factor cuts of a 25-element linear array using the 1D representation: (a) Exact phase and (b) 3-bit phase shifters*

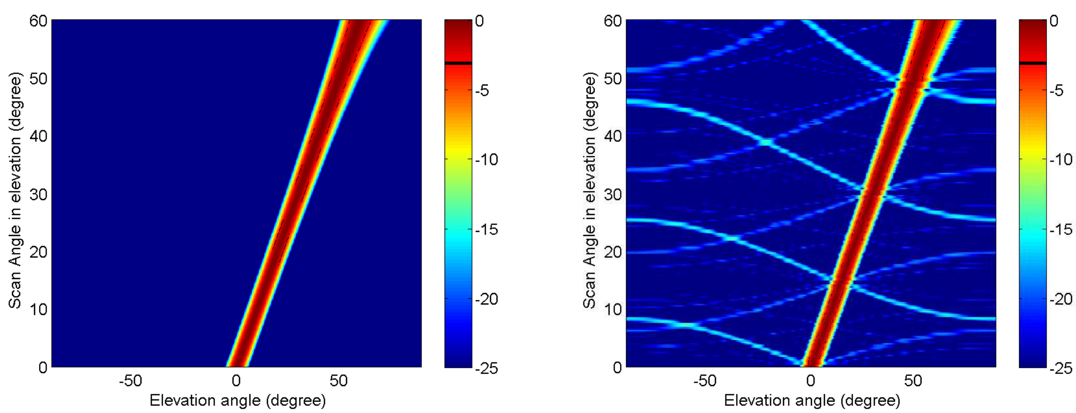

(a) (b)

Figure 3: *Array factor cuts of a 25-element linear array using the 2D colour representation: (a) Exact phase and (b) 3-bit phase shifters*

3 Results with perfect phase

The array factors of a linear antenna array set up with ideal phase shifters are presented in this section as a function of the null position. These results will be used later on as a reference to evaluate the performance with digital phase shifters.

3.1 General overview of the synthesized array factor as a function of the null position

The variation in the array factor as a function of the null position is addressed in this section considering a 16-element linear array. The 2D colour representation will be used here as it is convenient to have a global picture of the array factor depending on the null position and to make some comparisons with the Array Factor Without Prescribed Null (AFWPN). The AFWPN will be the reference array factor in this study.
Figure 4 shows the AFWPN for a uniform excitation in amplitude and phase using the 1D and 2D colour representations. The Half-Power Beamwidth (HPBW) is 6.4°, and the sidelobe and natural null positions are indicated in Table 1.

Sidelobe (°)	± 10.4	± 18	± 25.8	± 34	± 43.2	± 53.2	± 69.6	
Natural null (°)	± 7.2	± 14.4	± 22	± 30	± 38.6	± 48.6	± 61	± 90

Table 1: *Sidelobe and natural null positions in the array factor of a 16-element linear array with a constant half-wavelength element spacing*

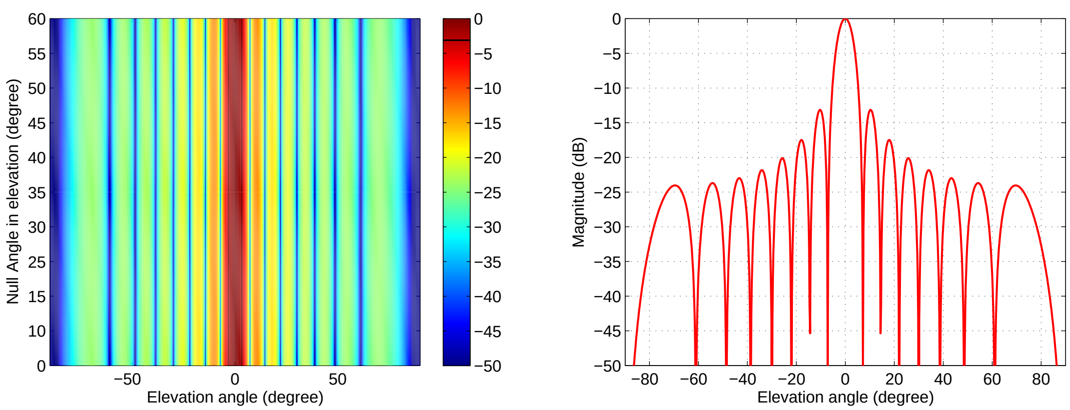

(a) (b)

Figure 4: *Array factor of a 16-element array without prescribed null: (a) 2D colour and (b) 1D representations*

Keeping the main beam at boresight and adding a null scanning from 1 to 60° in elevation, the 2D colour representation of figure 5 is obtained by calculating the weights at each element for each direction using the Applebaum method. The left hand-side of the array factor is similar to the one without prescribed null. However, the right hand-side shows the nulls disposed along a diagonal line containing some “nodes” formed by the intersection of the natural null and the prescribed null positions.

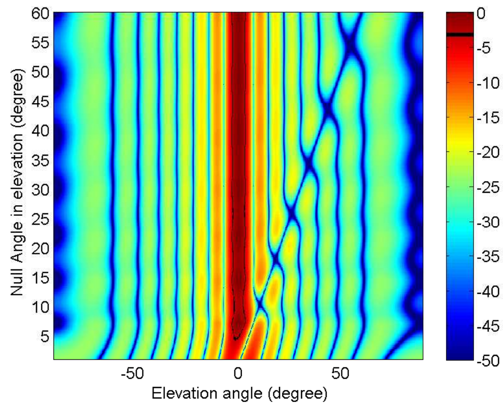

Figure 5: *Array factor of a 16-element array with a null varying from 1 to 60° in elevation*

To see the tendency of the array factor as a function of the null position, three cases have been selected to plot the 1D representation and to look at its main feature. The first case is when the null is relatively close to the main beam ($\theta_{null} = 3°$), the second one is for a null located in the direction of a natural null of the AFWPN ($\theta_{null} = 22°$), and the last case is for a null in the direction of a sidelobe of the AFWPN ($\theta_{null} = 34°$).

If the null is set up close to the main beam, two effects occur (Fig. 6):

- the direction of the main beam is shifted,
- the main beam is split, and as a result an additional sidelobe appears.

When the null is steered in the direction of a natural null of the AFWPN, the array factor is very similar to the one without prescribed null (Fig. 7). In the 2D colour representation (Fig. 7(a)), the position of the null along the diagonal is located half way between two “nodes”.

Finally, for a null set up in the direction of a sidelobe of the AFWPN, the steered null is wide (Fig. 8) compared to the previous case. In the 2D colour representation (Fig. 8(a)), the position of the null along the diagonal corresponds to a “node”.

Following this overview of the change in the array factor as a function of the null position, detailed characteristics of the main beam and the prescribed null are presented in Section 3.2.

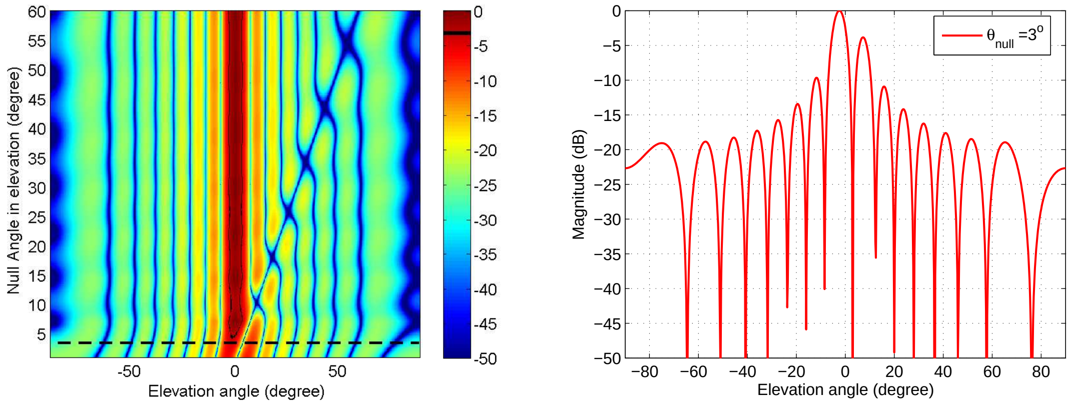

(a) (b)

Figure 6: *Array factor of a 16-element array with a null varying from 1 to 60° in elevation: (a) 2D colour and (b) 1D representations for* $\theta_{null} = 3^\circ$.

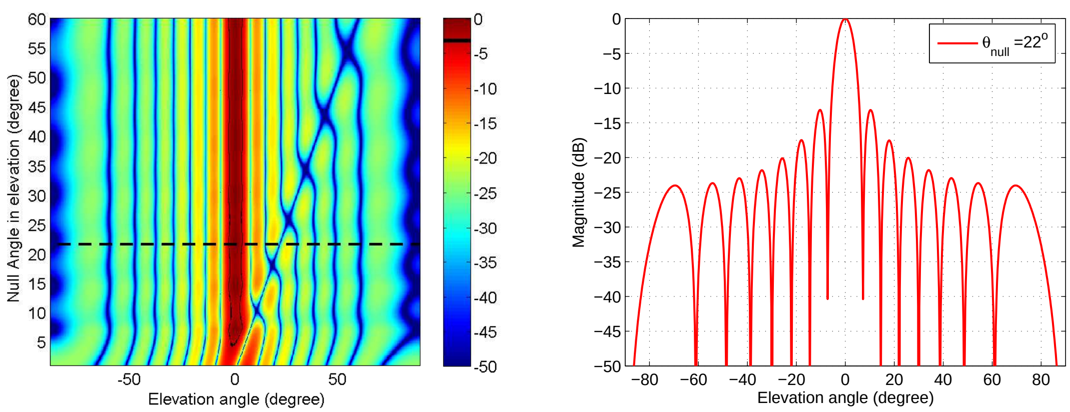

(a) (b)

Figure 7: *Array factor of a 16-element array with a null varying from 1 to 60° in elevation: (a) 2D colour and (b) 1D representations for* $\theta_{null} = 22^\circ$.

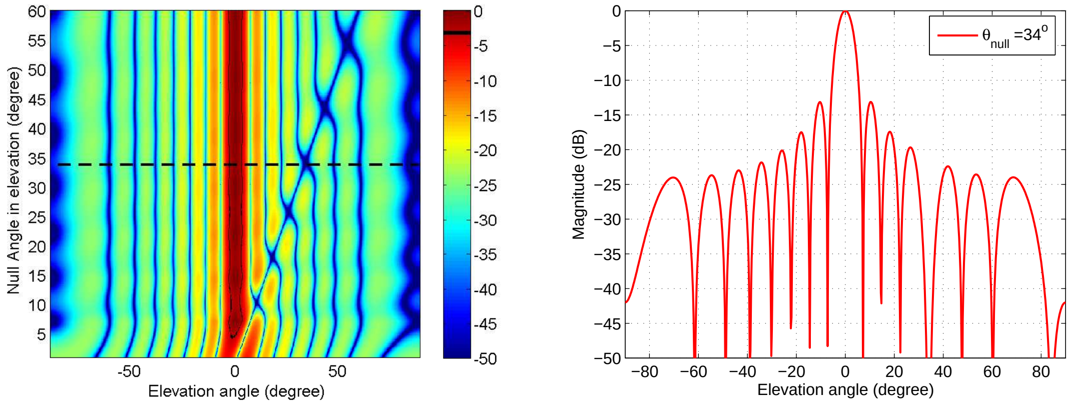

(a) (b)

Figure 8: *Array factor of a 16-element array with a null varying from 1 to 60° in elevation: (a) 2D colour and (b) 1D representations for* $\theta_{null} = 34°$.

3.2 Characteristics of the main beam and the prescribed null with perfect phase

Based on the array factor results presented in section 3.1, the characteristics of the main beam and the prescribed null can be extracted. Detailed features of these latter are addressed in this sub-section.

3.2.1 Angular position and half-power beamwidth of the main beam

Figure 9 shows the beam angular position and half-power beamwidth of the beam as a function of the null position. One can observe in Fig. 9(a) that the direction of the main beam is shifted when the prescribed null position is lower than the first natural null (7°) of the AFWPN. This agrees with the comments on the first case of Section 3.1, and moreover defines the threshold bellow which the prescribed null position affects the main beam. The position of the threshold corresponds to the point where the beam angular position reaches the desired value, here 0°. Similarly, it is seen that the HPBW of the main beam drops when the null position is below a threshold defined the same way as for the beam position (Fig. 9(b)).

3.2.2 Prescribed null depth

The plot of the null depth as a function of the prescribed null position presents maxima and minima as seen in Fig. 10(a). By superposing the null depth plot with the AFWPN, one can see that these maxima and minima correspond to the sidelobes and natural nulls of the

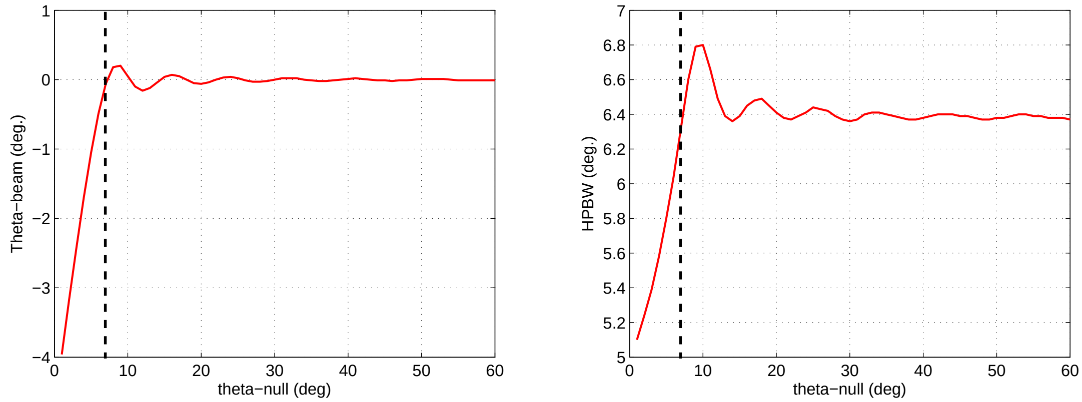

(a) (b)

Figure 9: *Main beam characteristics for a 16-element array with a null varying from 1 to 60° in elevation: (a) Beam angular position and (b) half-power beamwidth*

AFWPN, respectively.

As seen for the beam characteristics, the appearance of the prescribed null depth's curve confirms the comments made in Section 3.1. In particular, it is interesting to keep in mind that the array factor presents a wider null when the prescribed null direction corresponds to the angular position of a sidelobe, and that the array factor is very similar to the one without prescribed null if the prescribed null direction coincides with the angular position of a natural null.

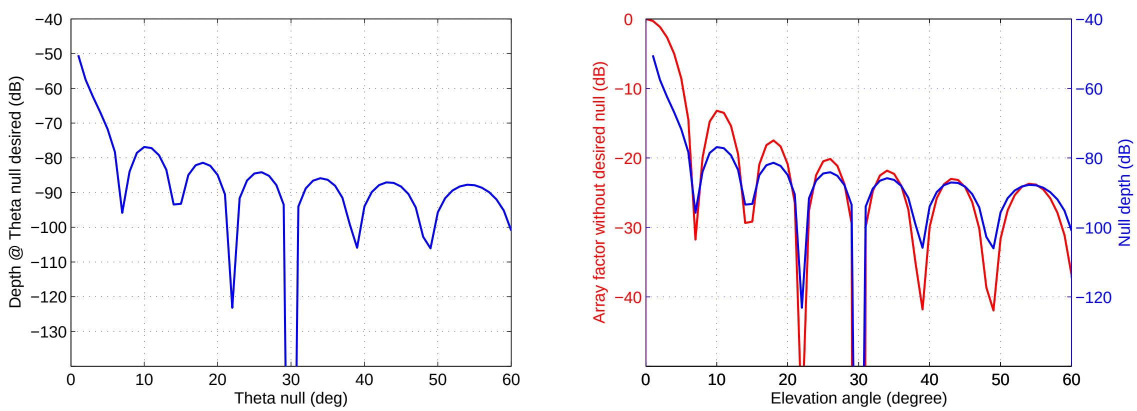

(a) (b)

Figure 10: *Prescribed null characteristics for a 16-element array with a null varying from 1 to 60° in elevation: (a) Prescribed null depth and (b) Superposition of the array factor without prescribed null and the prescribed null depth*

The results presented so far have been obtained considering a 16-element linear array. In Section 3.3, larger linear arrays are investigated to evaluate the effect on the null depth.

3.3 Effect of the sidelobe level in the array factor without prescribed null on the null depth

The envelope of the null depth maxima as a function of the prescribed null position is shown in Fig. 11(a). One can observe that the null depth maxima are decreasing when the number of elements increases. It is interesting to compare these maxima to the envelope of the sidelobe level of an array without prescribed null in Fig. 11(b). From these two plots, it is obvious that the sidelobe level of the AFWPN is correlated to the null depth.

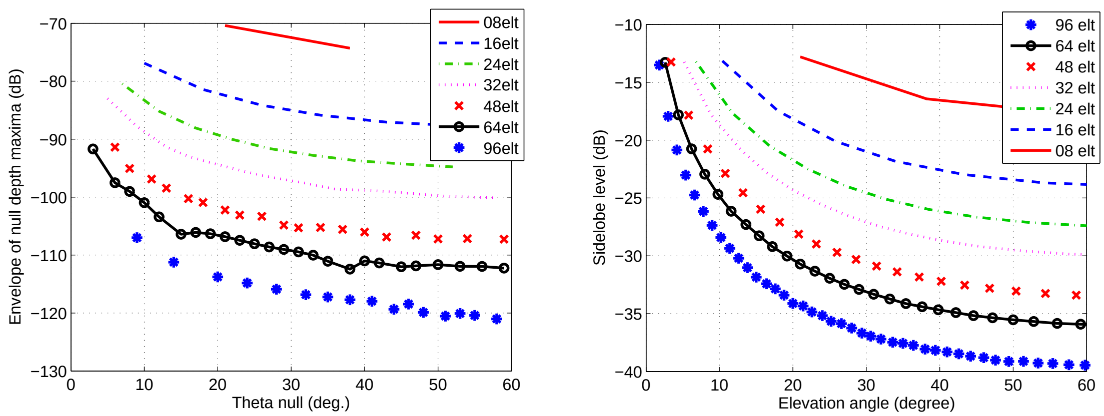

(a) (b)

Figure 11: *(a) Envelope of null depth maxima and (b) Sidelobe envelope for different array sizes with a null varying from 1 to 60° in elevation*

Another way to see this is to use sidelobe level reduction. Considering a 16-element linear array, Chebyshev amplitude distributions have been employed to compute the null depth for a null varying from 1 to 60° in elevation. Fig. 12(a) shows the null depth as a function of the null position for sidelobes with uniform distribution, and Chebyshev 20, 30 and 40 dB amplitude distribution. The lower the sidelobes, the deeper the nulls. Fig. 12(b) presents an enlargement for null position between 0 and 15° where it is noticeable that the position of the first null minimum shifts when the sidelobes are dropping. This comes from the fact that sidelobe reduction leads to an increase of the main beam HPBW, and thus the first natural null of the AFWPN is shifted.

Plotting the main lobe HPBW, the null angular position thresholds related to the different amplitude distribution can be defined. As a reminder, the main beam direction is shifted if the prescribed null position is set up below the threshold value. Fig. 13 shows the different threshold values depending on the particular amplitude distribution.

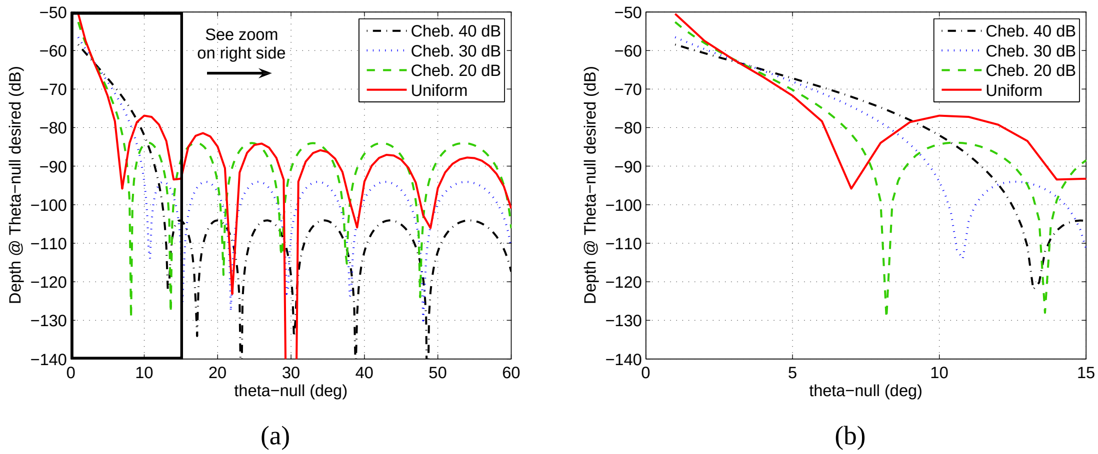

Figure 12: *Prescribed null depth for a 16-element array using Chebyshev amplitude distribution with a null varying from 1 to 60° in elevation: (a) Elevation from 0 to 60° and (b) Elevation zoomed between 0 and 15°*

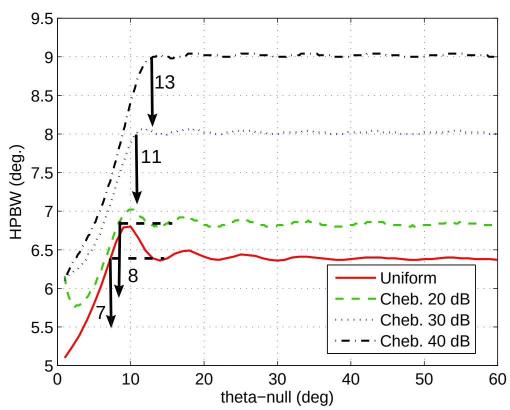

Figure 13: *Half-power beamwidth of the main beam for a 16-element array using Chebyshev amplitude distribution with a null varying from 1 to 60° in elevation*

3.4 Concluding remarks

Considering a 16-element linear array set up with ideal phase shifters, the characteristics of the array factor as a function of the null position has been addressed in this section for a prescribed null varying between 1 and 60°. The important outcomes are the following:

- The main beam angular position is shifted and the HPBW drops when the prescribed null is below the position of the first natural null of the AFWPN,
- The prescribed null depth curve presents some maxima and minima whose angular positions correspond to the sidelobes and natural null of the AFWPN, respectively. In particular, the prescribed null is wider but less deep when its angular position coincides with a sidelobe than for a natural null direction.

These results will be used in Section 4 as a reference to evaluate the effect of phase quantization.

4 Effect of phase quantization on the main beam and the prescribed null characteristics

The effect of having discrete phase instead of exact phase is investigated in this section. The considered criteria, an overview of the variation in the array factor, and the beam and lobe characteristics are reported here.

4.1 Criteria used to investigate the effect of phase quantization

A usual way to investigate the phase quantization effect is to use the Root Mean Square Error (RMSE) of the phase. For each prescribed null angle, the RMSE of the phase is calculated by:

$$RMSE = \sqrt{\frac{1}{N} \cdot \sum_{i=1}^{N} PhaseErr(i)^2} \tag{4.1}$$

where N is the number of array elements and $PhaseErr = \psi_m - \psi_{m\ discr.}$ is the phase error defined as the difference between the exact and the discrete phase.
To illustrate the RMSE of the phase, a 6-bit digital phase shifter can be considered for instance. The corresponding phase RMSE is presented in Fig. 14(a). One can notice that the phase RMSE is close to zero at the natural null positions of the AFWPN (Fig. 14(b)). To explain this, the RMS of the exact phase is plotted in Fig. 15(a) using equation (4.2). This curve shows that the phase RMS is equal to zero at the natural null angles of the AFWPN. The RMS of the exact amplitude as a function of the prescribed null directions is given in Fig. 15(b), and similarly this curve shows that the amplitude RMS is equal to one at the natural null angular positions. This means that the AFWPN is unchanged for prescribed null at the natural null positions since the array weights are equal to 1 in amplitude and zero in phase when prescribed null are set at the natural null positions.

$$RMS = \sqrt{\frac{1}{N} \cdot \sum_{i=1}^{N} Phase(i)^2} \tag{4.2}$$

In this study, the prescribed null is varying from 1 to 60°. Because the phase RMSE is computed for each prescribed null angle, the average of the phase RMSE is considered for the whole set of prescribed null angles.

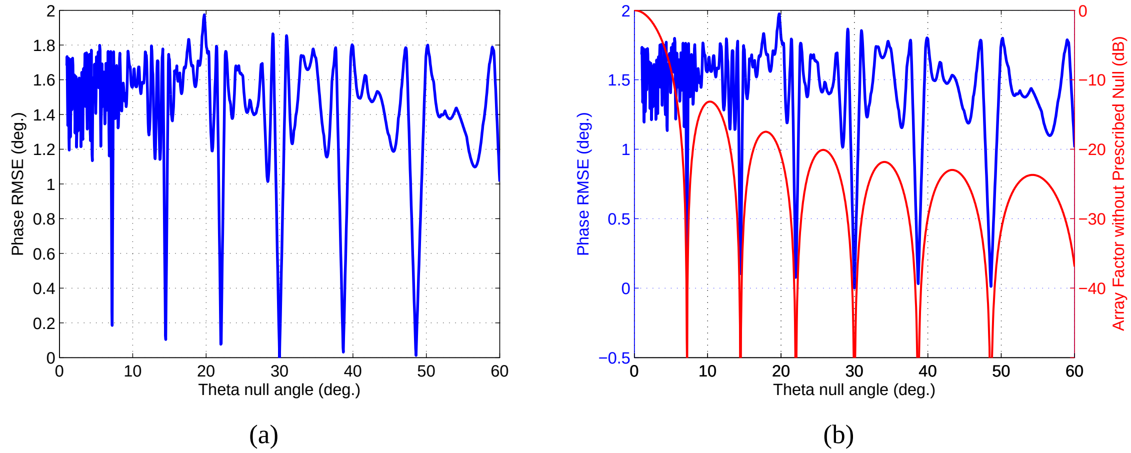

Figure 14: *Root mean square of the phase error for a 16-element array using a 6-bit digital phase shifter with a null varying from 1 to 60° in elevation: (a) RMSE of the phase, and (b) Superposition of the RMSE of the phase and the array factor without prescribed null.*

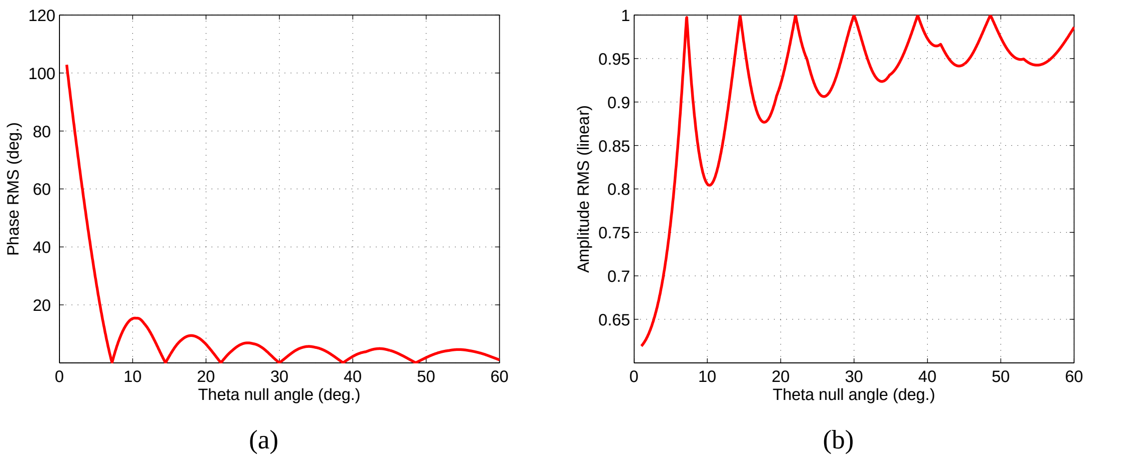

Figure 15: *Root mean square of the exact phase and amplitude for a 16-element array with a null varying from 1 to 60° in elevation: (a) RMS of the phase and (b) RMS of the amplitude.*

4.2 Overview of the phase quantization effect

Fig. 16 shows different array factors of a 16-element linear array with a prescribed null varying between 1 and 60° using the 2D colour representation. The synthesized array factor with exact phase is given in Fig. 16(a), and the array factor with different average phase RMSE values due to phase quantization are presented in Fig. 16(b), (c) and (d). When the average phase RMSE is small (0.4°), the difference between the array factor with exact phase and with phase error is negligible. For a moderate average phase error RMS (2.7°), one can notice that the prescribed null depth is reduced, as the diagonal formed by the prescribed null is not as clear as with perfect phase. Finally, the array factor is greatly affected in terms of the null angular position and the null depth when the average phase error RMS is large (6.2°). In Fig. 16(c) and (d), some elevations have more distortion than others because the phase is unchanged between two (or more) consecutive elevations due to the fact that the phase shifter number of bits is low (respectively 5 and 2 bits).

Subsequent to this overview, the main beam and prescribed null characteristics are examined in detail in Section 4.3.

4.3 Characteristics of the main beam and the prescribed null with phase quantization

Phase quantization deteriorates the performances of smart antenna systems. The main beam and prescribed null characteristics are analysed in this part as a function of the average phase RMSE for a 16-element linear array.

4.3.1 Angular position and half-power beamwidth of the main beam

Fig. 17 presents the main beam angular position and HPBW as a function of the average phase RMSE relative to the results obtained with exact phase. This means that each result is subtracted from the result obtained with perfect phase. Thus, the resulting curves represent the main beam position and HPBW error. One can notice that the direction and HPBW of the main beam are slightly different than the results with exact phase when the phase error is large.

As for digital beam-scanning, phase quantization does not affect significantly the main beam characteristics, except in the cases of large phase error.

4.3.2 Prescribed null angle and depth

In a similar way as for the main beam characteristics, the prescribed null angular position and depth error can be computed as a function of the average phase RMSE (Fig. 18).

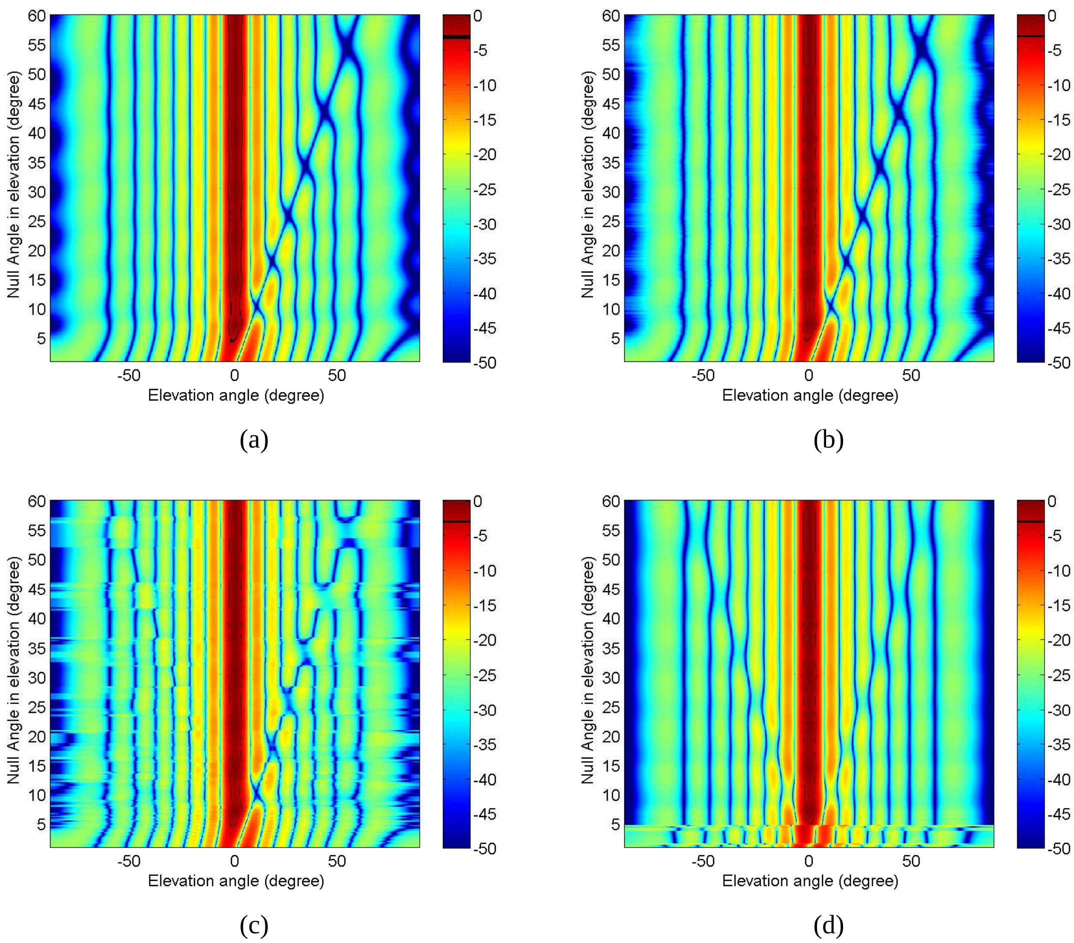

Figure 16: *Array factor of a 16-element linear array with a prescribed null varying from 1 to 60° in elevation using the 2D colour representation : (a) Exact phase, and with average phase RMSE of (b) 0.4°, (c) 2.7°, and (d) 6.2°*

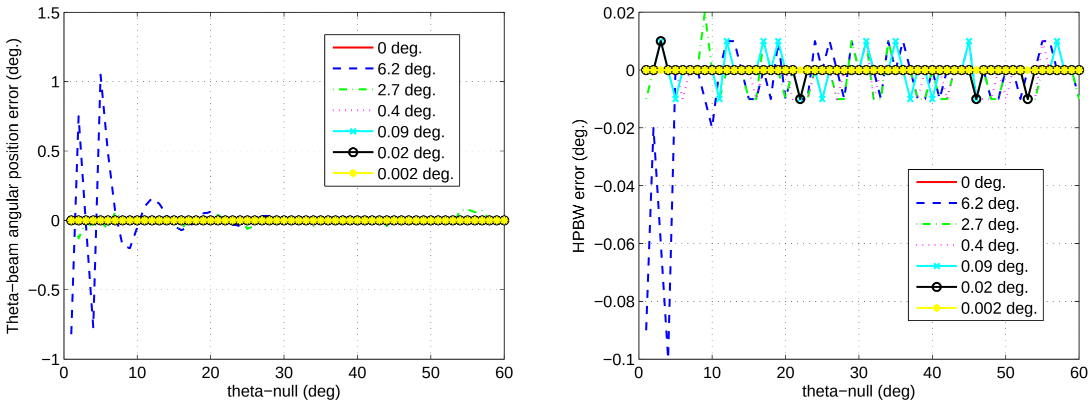

(a) (b)

Figure 17: *Phase quantization effect on the main beam characteristics for a 16-element linear array with a prescribed null varying from 1 to 60° in elevation: Main beam (a) Angular position, and (b) HPBW.*

In this case, the position and depth of the prescribed null are both affected by the phase quantization. The larger the phase error, the higher the effect. For instance, the prescribed null angular position can present an error up to 4.4° and the null depth an error around 60° when the average phase error RMS is 6.2°.

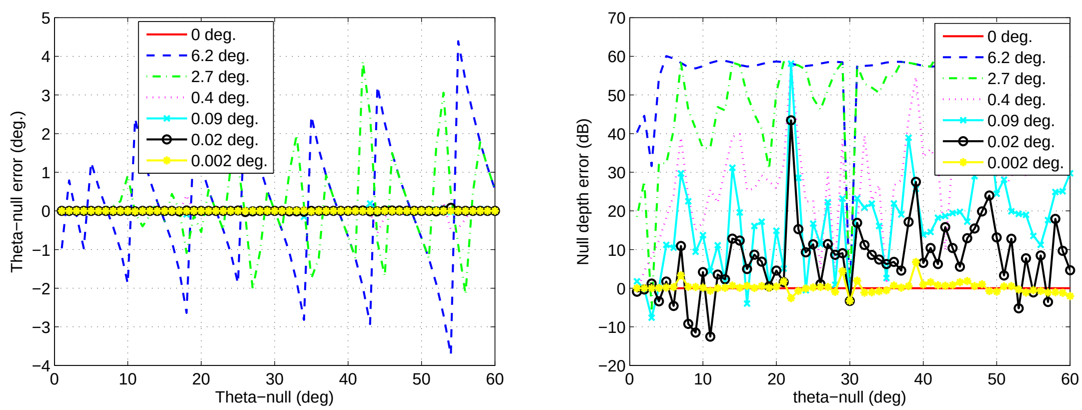

(a) (b)

Figure 18: *Phase quantization effect on the prescribed null characteristics for a 16-element linear array with a prescribed null varying from 1 to 60° in elevation: (a) Relative error angle, and (b) depth error.*

5 Conclusions and future work

Investigations into the radiation characteristics of linear arrays with half-wavelength element spacing and digital phase shifters have been reviewed in this report for an array factor having a main beam and a prescribed null. The weights of each element have been computed using the Minimum Variance Distorsionless Response method. In the considered scenario, the main beam is fixed and the prescribed null angular position varies between 1 and 60°.

Different results have been presented, first for exact phase and different number of elements. The main beam angular position is shifted and the HPBW drops when the prescribed null is below the position of the first natural null of the array factor without prescribed null. The prescribed null depth curve presents some maxima and minima whose angular positions correspond to the sidelobes and natural null of the array factor without prescribed null, respectively. Additionally, the array factors having a prescribed null corresponding to the natural null positions are very similar to the synthesized array factor without prescribed null. Indeed, the array element weights are equal to 1 in amplitude and zero in phase in these cases. Moreover, the depth envelope of the prescribed null maxima is related to the level of the sidelobes of the array factor without prescribed null.

Based on these facts, the effect of phase quantization has been studied. In particular, it has been observed that the main beam angular position and half-power beamwidth errors are negligible. However, phase quantization affects the prescribed null position and depth. The larger the phase error, the greater the effect on the radiation pattern characteristics.

The investigation of phase quantization effects for arrays of various geometries as well as multiple beams and nulls is planned for future work. Only linear arrays have been considered in this study and it would be interesting to obtain results considering other array geometries. The same is true of multiple beams and nulls since one beam and one null have been investigated here, and realistic scenarios assume more than one beam and/or null.

References

[1] H. Steyskal, R. A. Shore and Haupt, R. L. (1986), Methods for Null Control and their Effects on the Radiation Pattern, *IEEE Trans. Antennas Propagat.*, 34(3), 404–409.

[2] Hicks, D. S. (1977), Null steering in linear arrays by using amplitude control of signals in the feeder network, *Electronics Letters*, 13(7), 198–199.

[3] Liao, W.-P. and Chu, F.-L. (1997), Null steering in planar arrays by controlling only current amplitudes using genetic algorithms, *Microwave and Optical Technology Letters*, 16(2), 97–103.

[4] Ananasso, F. (1981), Nulling performance of null-steering arrays with digital phase-only weights, *Electronics Letters*, 17(7), 255–257.

[5] Applebaum, S. P. (1976), Adaptive Arrays, *IEEE Trans. Antennas Propagat.*, 24(5), 585–598.

[6] Ismail, T. H. and Dawoud, M. M. (1991), Null steering in phased arrays by controlling the element positions, *IEEE Trans. Antennas Propagat.*, 39(11), 1561–1566.

[7] Gupta, I. J. (1986), SMI Adaptive Antenna Arrays for Weak Interfering Signals, *IEEE Trans. Antennas Propagat.*, 34(10), 1237–1242.

[8] Rogojan, S. and Clénet, M. (2006), PAASoM User Guide, Release 1, *Defence R&D Ottawa, DRDC Ottawa SL 2006-213*.

[9] Clénet, M. and Morin, G. A. (2003), Visualization of Radiation Pattern Characteristics of Phased Arrays Using Digital Phase Shifters, *IEEE Antennas Propagat. Magazine*, 45(2), 20–35.

[10] Clénet, M. and Martel, P. (2007), Update on the Development of a Phased Array Antenna Simulation Tool, *URSI International Symposium on Electromagnetic Theory (EMTS), Ottawa, ON*.

[11] Jr., R. T. Compton, The Power-Inversion Adaptive Array: Concept and Performance, *IEEE Trans. Aerosp. Electron. Syst.*, 15(6), 803.

DOCUMENT CONTROL DATA

(Security classification of title, body of abstract and indexing annotation must be entered when document is classified)

1. ORIGINATOR (The name and address of the organization preparing the document. Organizations for whom the document was prepared, e.g. Centre sponsoring a contractor's report, or tasking agency, are entered in section 8.) Defence R&D Canada – Ottawa 3701 Carling Avenue Ottawa, Ontario K1A 0Z4 Canada	2. SECURITY CLASSIFICATION (Overall security classification of the document including special warning terms if applicable.) UNCLASSIFIED

3. TITLE (The complete document title as indicated on the title page. Its classification should be indicated by the appropriate abbreviation (S, C or U) in parentheses after the title.)

Study of phase quantization effects on synthesized array factor having a main beam and a prescribed null

4. AUTHORS (Last name, followed by initials – ranks, titles, etc. not to be used.)

Caillet, M.; Clénet, M.; Antar, Y.M.M.

5. DATE OF PUBLICATION (Month and year of publication of document.) December 2008	6a. NO. OF PAGES (Total containing information. Include Annexes, Appendices, etc.) 34	6b. NO. OF REFS (Total cited in document.) 11

7. DESCRIPTIVE NOTES (The category of the document, e.g. technical report, technical note or memorandum. If appropriate, enter the type of report, e.g. interim, progress, summary, annual or final. Give the inclusive dates when a specific reporting period is covered.)

Technical Memorandum

8. SPONSORING ACTIVITY (The name of the department project office or laboratory sponsoring the research and development – include address.)

Defence R&D Canada – Ottawa
3701 Carling Avenue
Ottawa, Ontario K1A 0Z4 Canada

9a. PROJECT NO. (The applicable research and development project number under which the document was written. Please specify whether project or grant.) 15en01	9b. GRANT OR CONTRACT NO. (If appropriate, the applicable number under which the document was written.)
10a. ORIGINATOR'S DOCUMENT NUMBER (The official document number by which the document is identified by the originating activity. This number must be unique to this document.) DRDC Ottawa TM 2008-291	10b. OTHER DOCUMENT NO(s). (Any other numbers which may be assigned this document either by the originator or by the sponsor.)

11. DOCUMENT AVAILABILITY (Any limitations on further dissemination of the document, other than those imposed by security classification.)

(X) Unlimited distribution
(   ) Defence departments and defence contractors; further distribution only as approved
(   ) Defence departments and Canadian defence contractors; further distribution only as approved
(   ) Government departments and agencies; further distribution only as approved
(   ) Defence departments; further distribution only as approved
(   ) Other (please specify):

12. DOCUMENT ANNOUNCEMENT (Any limitation to the bibliographic announcement of this document. This will normally correspond to the Document Availability (11). However, where further distribution (beyond the audience specified in (11)) is possible, a wider announcement audience may be selected.)

Unlimited

13. ABSTRACT (A brief and factual summary of the document. It may also appear elsewhere in the body of the document itself. It is highly desirable that the abstract of classified documents be unclassified. Each paragraph of the abstract shall begin with an indication of the security classification of the information in the paragraph (unless the document itself is unclassified) represented as (S), (C), (R), or (U). It is not necessary to include here abstracts in both official languages unless the text is bilingual.)

This document reports on investigations into the radiation characteristics of linear arrays with half-wavelength element spacing and digital phase shifters for an array factor having a main beam and a prescribed null. The weights of each element have been computed using the Minimum Variance Distorsionless Response method. In the considered scenario, the main beam is fixed and the prescribed null angular position varies between 1 and 60°.

Different results are presented here, first for exact phase and different number of elements. The main beam angular position is shifted and the half-power beamwidth drops when the prescribed null is below the position of the first natural null of the array factor without prescribed null. The prescribed null depth curve presents maxima and minima whose angular positions correspond to the sidelobes and natural nulls of the array factor without prescribed null, respectively. Moreover, the depth envelope of the prescribed null maxima is related to the level of the sidelobes of the array factor without prescribed null.

Based on these facts, the effect of phase quantization are studied. In particular, one can observe that the main beam angular position and half-power beamwidth errors are negligible. However, phase quantization affects the prescribed null position and depth. The larger the phase error, the greater the effect on the radiation pattern characteristics.

14. KEYWORDS, DESCRIPTORS or IDENTIFIERS (Technically meaningful terms or short phrases that characterize a document and could be helpful in cataloguing the document. They should be selected so that no security classification is required. Identifiers, such as equipment model designation, trade name, military project code name, geographic location may also be included. If possible keywords should be selected from a published thesaurus. e.g. Thesaurus of Engineering and Scientific Terms (TEST) and that thesaurus identified. If it is not possible to select indexing terms which are Unclassified, the classification of each should be indicated as with the title.)

Array signal processing, digital circuits, phase shifters, quantization, interference suppression

Defence R&D Canada

Canada's leader in Defence
and National Security
Science and Technology

R & D pour la défense Canada

Chef de file au Canada en matière
de science et de technologie pour
la défense et la sécurité nationale

DEFENCE R&D DÉFENSE

www.drdc-rddc.gc.ca